Myeloperoxidase loss protects against delayed cerebral injury after subarachnoid hemorrhage

Aminata P. Coulibaly[1]; Pinar Pezuk[1]; William Gartman[1,3]; Danielle Triebwasser[1]; J. Javier Provencio[1,2]

Department of Neurology[1], Department of Neuroscience[2], University of Virginia Charlottesville, Virginia; University of North Carolina Chapel Hill[3].

Aminata P Coulibaly: apc6s@virginia.edu

Pinar Pezuk: ppzuk@gmail.com

William Gartman: willgartman@gmail.com

Danielle Triebwasser: djt2vr@virginia.edu

J. Javier Provencio: jpb3@virginia.edu

Corresponding author:

J. Javier Provencio, MD

Louise Nerancy Associate Professor in Neurology and Neuroscience

Email: JP3B@virginia.edu

Office number: (434)297-7608

Abstract

Background: Neutrophil infiltration into the central nervous system (CNS) after aneurysmal subarachnoid hemorrhage (SAH) is critical to the development of delayed cerebral injury (DCI). The goal of the present study is to characterize the neutrophil activity that leads to DCI.

Methods: We tested mice deficient in elastase, NADPH oxidase, or myeloperoxidase (MPO) in our SAH model for delayed spatial memory changes and vascular constriction associated with DCI. Because the MPO mouse showed no DCI, we focused on the MPO null mice, including experiments to reconstitute the MPO effect by injection of active MPO and its substrate, H_2O_2. Flow cytometry and immunohistochemistry were used to determine the temporal and spatial location of neutrophils and glial cells in the CNS after SAH in WT and MPO null mice.

Results: Following SAH, neutrophils infiltrate the outer meninges from outside the CNS in a delayed fashion. Mice with functional deletion of the neutrophil effector molecule myeloperoxidase (MPO KO) do not develop DCI. Re-introduction of biologically active MPO to the meninges, i.e. CSF, of MPO KO mice at the time of the hemorrhage restores the spatial memory deficit seen in DCI. However, addition of active MPO to the CSF of wildtype mice (WT) without hemorrhage does not lead to DCI, suggesting that blood components and MPO are necessary to cause DCI in our model. The localization of neutrophils, exclusively in the meninges, suggests that their effect on spatial memory goes through intermediate cells (presumably glia). Astrocyte reactivity increases in WT after SAH but not in MPO KO mice, suggesting that astrocytes mediate the effects of neutrophil-derived MPO on neurons in the brain parenchyma after SAH.

Conclusions: These results demonstrate that neutrophils can modulate cognition from the meninges, and that immune cell reactivity in the meninges can modulate spatial memory through indirect effects on neurons.

Keywords: Innate Inflammation; myeloperoxidase; neutrophil; aneurysmal subarachnoid hemorrhage; meningeal inflammation; spatial memory.

Background

The role of peripheral neutrophils in the central nervous system (CNS) during sterile injury is poorly understood. Infiltration of neutrophils into the CNS has been associated with neuronal damages in a number of disease and injury models[1–4]. In models of Parkinson's Disease, neutrophil infiltration increases the loss of dopaminergic neurons in the substantia nigra pars compacta [2]. Following focal ischemia, neutrophil infiltration of the brain parenchyma correlates with the onset of cognitive deficits[1]. In our model of mild subarachnoid hemorrhage (SAH), the presence of neutrophils in the CNS is critical to the development of late cognitive deficits [5,6]. In fact, the presence of neutrophils in the CNS seems to be detrimental to brain physiology and functional output. Our laboratory is interested in determining the mechanism through which neutrophils affect neuronal activity during inflammation.

Neutrophils recruited to a site of infection or injury release specific molecules that fall into three general classes: enzymes that catalyze the development of reactive oxygen and nitrogen species, enzymes that catalyze the degradation of extracellular matrix proteins, and proteins that bind cell surface receptors [7,8]. A few of these molecules are implicated in brain tissue damage after injury. Inhibition of neutrophil enzymes myeloperoxidase and elastase reduce oxidative stress in a mouse model of cerebral ischemia [9,10]. The inhibition of NADPH oxidase, myeloperoxidase, and elastase decrease neuronal damage in mice after cerebral ischemia, traumatic brain injury, and spinal cord injury [9,11–13]. In this study, we evaluate the role of these three neutrophil enzymes in a mouse model of mild, sterile brain injury.

Subarachnoid hemorrhage (SAH) is a unique model of sterile brain injury. Unlike ischemic stroke, intraparenchymal hemorrhage, or trauma, the primary mechanism of damage is in the meninges not to the parenchyma of the brain, allowing for the evaluation of secondary brain injury. Our laboratory uses a model of mild subarachnoid hemorrhage from a venous source, which does not lead to increased intracranial pressure or direct brain damage. Indeed, mice show intact motor function after the hemorrhage [6]. In humans, SAH leads to a syndrome of delayed cerebral injury (DCI) characterized by a delayed development of cognitive deficits. These deficits have been documented in our model[6], giving us the unique opportunity to study the mechanisms leading to cognitive dysfunction.

Innate inflammatory cells, particularly neutrophils, are recruited into the CNS 3 days after the hemorrhage[6]. These cells play a critical role in the development of DCI. In patients, after SAH, neutrophil infiltration in the cerebrospinal fluid (CSF) precedes DCI[14]. CSF from SAH patients applied to a skinfold chamber in mice facilitates microvascular recruitment of innate immune cell and precipitate vasospasm in mice [15]. Additionally, blockage of the integrin CD11/CD18a, a molecule complex critical for innate immune cell extravasation, prevents vasospasm. In fact, depletion of neutrophils from the peripheral blood 3 days after hemorrhage prevents the development of DCI in mice[5]. Here, we hypothesis that neutrophil activity, through its release of granular enzymes, is critical to the development of DCI. Our results show that neutrophil infiltration in the CNS after a mild SAH is restricted to the meningeal space and that the activity of its enzyme, myeloperoxidase is critical to the development to of DCI. Furthermore, we demonstrate that neutrophil action on neurons after SAH is through its modulation of astrocyte physiology and function.

Methods

Animals

Young (8-12 weeks old) male mice were used in all experiments. Mice were kept on a 12 hour:12-hour light cycle at room temperature (22-25°C). Food and water were provided *ad libitum*. All experiments were done with the approval of the University of Virginia Animal Care and Use Committee.

Transgenic mice deficient in the enzymes elastase (B6.129X1-Elane tm1sds: elastase KO), myeloperoxidase (B6.129X1-Mpo tm1Lus: MPO KO) or neutrophil cytosolic factor 1(NCF-component of the NADPH oxidase complex (B6(Cg)-Bcf1 m1J: NADPH oxidase KO) (The Jackson Laboratories) were used. All transgenic mice used were on a C57BL/6 background; therefore, control experiments were conducted on C57BL/6J mice. Of note, the number of mice used in each of the subsequent experiments is listed in Table 1.

Flow Cytometry	Vasospasm	IHC	Barnes Maze	Open Field	Novel object Recognition	Rotarod
WT Naïve = 8 Sham = 20 SAH = 19	**WT** Sham = 8 SAH = 7	**WT** Naïve = 6 Sham = 28 SAH = 29	**WT** Naïve = 6 Sham =23 SAH = 8	**WT** Sham = 32 SAH = 8	**WT** Sham = 32 SAH = 8	**WT** Naïve = 6
MPO KO Naïve = 5 Sham = 6 SAH= 5	**MPO KO** Sham = 6 SAH = 6	**MPO KO** Sham = 18 SAH = 20	**MPO KO** Naïve = 6 Sham = 13 SAH = 37	**MPO KO** Sham = 7 SAH = 23	**MPO KO** Sham = 8 SAH = 22	**MPO KO** Naïve = 5
			Elastase KO Sham = 7 SAH = 9			
			NADPH Oxidase KO Sham = 11 SAH = 12			

Table 1: Number of mice used in each experiment

Subarachnoid hemorrhage (SAH)

SAH or sham surgeries were performed as previously reported [16]. Briefly, mice were anesthetized using isoflurane, and placed in a prone position. A 3mm incision was made on the back of the neck along the midline, the atlanto-occipital membrane was entered, and a conserved subarachnoid vein punctured. Bleeding from the vein was allowed to stop on its own. For the sham experiment, the procedure was the same except the atlanto-occipital membrane was not entered and the vein was not punctured.

Myeloperoxidase (MPO) injection

Wildtype (WT) and MPO KO mice received intracisternal injections of MPO enzyme, H_2O_2 or MPO with H_2O_2 in the setting of SAH or sham. Biologically active MPO (ab91116; Abcam, Cambridge, MA, US) was reconstituted in phosphate buffer saline (PBS) to a stock concentration of 1 µg/µl. MPO production of hydroclorous acid (HOCl) requires a H_2O_2 concentration of 0.0012% per unit of activity. Mice were given an injection with either 0.8 µg of MPO, 0.8 µg MPO with 0.0012% H_2O_2 in PBS, or 0.0012% H_20_2 in PBS at the time of surgery.

CD45-FITC injection

Mice were injected with 3 µg of anti-CD45-FITC antibody (Thermofisher, Waltham, MA, US) intravenously 30 minutes prior to euthanasia. Mice were then perfused with PBS and 4% paraformaldehyde. Meninges were dissected, stained for neutrophils with the anti-neutrophil antibody 7/4-FITC (Abcam, Cambridge, MA, US; 1:100), and imaged using an Olympus FV1200 confocal microscope and Fluoview software.

Flow cytometry

Flow cytometry was performed on both the brain parenchyma and meninges of SAH and sham operated mice. To generate a single cell suspension for flow cytometry, the meninges were collected and processed as previously described [17]. Briefly, meninges were dissected and processed in DMEM media with 10% bovine serum albumin (BSA). Samples were digested using 1 mg/ml DNAse and 1.4 U/ml collagenase in Hanks Balanced Salt Solution with magnesium and calcium. Samples were then incubated in a 37°C water bath, triturated and strained through a 70 µm cell filter. Samples were then centrifuged and resuspended in DMEM media with 10% BSA and kept on ice until staining. Once single cell suspensions were obtained, samples were blocked with Fc block and incubated with an antibody cocktail containing Ly6G-FITC, Ly6C-PeCy7, CD11b-efluor 780 (Life Technologies, Carlsbad, CA, US; 1:200), and CD45-Pacific blue (Biolegend, San Diego, CA, US; 1:200) for 30 minutes at 4ºC. To determine cell viability within each suspension, an aliquot of each sample was incubated with the fixable viability dye efluor 506 (ThermoFisher, Waltham, MA, US; 1:1000) for 30 minutes at 4ºC. Samples were then analyzed using a Gallios cytometer (Beckman Coulter, Brea, CA, US), and analyzed using FlowJo software (FlowJo, LLC, Ashland, OR, US).

Immunohistochemistry (IHC)

Mice were transcardially perfused with 4% paraformaldehyde in PBS. Brains and meninges were dissected and processed separately for immunohistochemistry. Brains were post-fixed in 4% paraformaldehyde for 24 hours followed by cryoprotection in a 30% sucrose solution. Brains were then frozen and 30 µm sections collected using a cryo-microtome. Sections containing the hippocampus were selected, rinsed in PBS, and blocked in a 0.3% TritonX with 5% normal goat

serum solution. Sections were then incubated with rabbit anti-Iba1 (Wako Chemicals, Japan 1:500), goat anti-Iba1 (Abcam, Cambridge, MA, US; 1:500), anti-neutrophil antibody 7/4-FITC (anti-Ly6B) (Abcam Cambridge, MA, US; 1:100), chicken anti-GFAP (Abcam, Cambridge, MA, US; 1:1000), rabbit anti-vimentin (Abcam, Cambridge, MA, US; 1:200), and rabbit anti-4HNE (Abcam, Cambridge, MA, US; 1:200) overnight at room temperature. The following day, sections were rinsed and incubated with AlexaFluor conjugated secondary antibody (ThermoFisher Scientific, Waltham, MA, US; 1:500) for 1 hour at room temperature, mounted on Superfrost Plus slides (ThermoFisher, Waltham, MA, US), and cover-slipped using Vectashield mounting medium with DAPI (Vector laboratories, Burlingame, CA, US).

Meninges were removed from the skullcap and kept in PBS until processing. Non-specific binding sites were blocked using PBS containing 1% BSA, 5% normal goat serum, 0.1% Triton-X, 0.2% tween, and Fc block. Meninges were then incubated in a primary antibody cocktail containing the anti-neutrophil antibody 7/4-FITC (Abcam, Cambridge, MA, US; 1:100) at 4ºC overnight.

Confocal image acquisition and analysis

All images were obtained on the Olympus FV1200 confocal microscope with Fluoview software. Each image was collected as a Z-stack. Prior to image analysis, all images were blinded and a maximum intensity image was generated by collapsing all stacks using ImageJ/Fiji (NIH, Bethesda, MD, US).

Brain: Images of both the left and right CA1 regions of the hippocampus was obtained using a 20x oil immersion objective. Composite images containing the nuclear marker DAPI and the cellular stain of interest (Iba1 for microglia and GFAP/vimentin for astrocytes) were then generated. Using the multipoint tool to isolate a region of interest (ROI), all of the cells within each image were counted. Counts for both left and right hippocampi were added and divided by two to generate an average number of cells per case. Using the 'Coloc 2' application for ImageJ/Fiji, a co-localization index for GFAP and Vimentin was obtained for each hippocampus. The values were averaged for left and right hippocampi to generate a value for each case.

Meninges: In order to image both the meninges containing the transverse sinus and the meningeal parenchyma (outer portion including dura mater and arachnoid membrane), whole mounts of the meninges were stained for neutrophils (NT 7/4; Abcam, Cambridge, MA, US). Using 20x oil immersion objective, a three by three tile was obtained of the transverse sinus and the meninges. Each image was obtained as a Z-stack. Prior to analysis, a maximum intensity image was obtained for each stack, and a DAPI and NT 7/4 composite was generated. For quantification, a nine by nine grid was placed on each image. From the left top square, six squares were counted (five horizontally and one vertically). Within the sixth square, the number of neutrophils were counted. A total of seven squares were counted per grid laid images for a total of 252 um^2 area (36 um^2 area/grid square) counted out of 4225 um^2 area (image size). The number of cells was then added across three by three tiled image (nine images per area), to generate a representative number of neutrophils present in each case.

Microglia Scholl analysis

Brain images of sections labelled with anti-iba1 antibody, were converted to 8-bit files. The iba1 fluorescence threshold of the images was set at 90% intensity, and a ten by ten grid was placed on each image. The fifth row of squares was cropped out and analyzed. Cells were only included in the analysis if fully located within the selected row. The 'Scholl analysis' application was then used to quantify the number of processes observed on selected cells using the protocol previously described [18].

Vasospasm

Previous studies from our lab show the presence of vascular spasm in the middle cerebral artery (MCA) of SAH mice early (at day 1) and, more importantly, in a delayed manner (6 days after the hemorrhage) corresponding to DCI in humans [6]. Since the peak neutrophil infiltration occurs in our model 3 days post-hemorrhage and delayed vasospasm is correlated with DCI, we focused our vasospasm analysis on the delayed vasospasm occurring on the 6^{th} day after SAH.

The arterial tree of each mouse was labeled using the vascular dye Microfil (Flow Tech, Carver, MA), and the cross-sectional MCA diameter was measured. Briefly, animals were anesthetized using sodium pentobarbital, transcardially perfused with 20 ml of cold PBS followed by 20 ml of cold 1% paraformaldehyde in PBS, then injected with 10 ml of Microfil dye. Brains were dissected, rinsed in PBS, then cleared using methyl salicylate (Sigma-Aldrich, St Louis MO US). The ventral surface of each brain was then imaged using a Leica DM 2000 LED light microscope. Because vasospasm leads to non-uniform constriction of arteries, there are affected and unaffected areas. The percent constriction was calculated as a ratio of the smallest diameter

to the largest cross-sectional diameter of the MCA within a 2 mm segment distal to the posterior wall of the internal carotid using ImageJ and converted to a percentage.

Behavior analysis

Barnes maze

Previous studies show that mice with SAH develop deficits in performance on the Barnes maze task 6-8 days after the hemorrhage[6]. Therefore, in the present study, this task was used to assess the presence of cognitive deficits after SAH. Briefly, mice were habituated to the maze for 2 days before the surgery. Habituation was performed by placing mice in the middle of the maze and leaving them to explore for 5 min. Testing started on day three post-surgery and continued for 9 consecutive days thereafter. During testing, mice were placed in the middle of the maze and given a total of 300 seconds to find the escape hole. Each trial ended when the mouse entered the escape hole, stayed in the vicinity of the escape hole (defined by a circle of 5 cm diameter around the escape hole) for 5 consecutive seconds, or the 300 second maximum had elapsed. All trials were recorded and analyzed using the tracking software Ethovision 13 (Noldus, Leesburg, VA, US).

Open field

To determine whether SAH and/or MPO injection caused anxiety-like behavior in mice, mice were allowed to freely explore a 45cm x 45cm box for 10 minutes. Using the behavior tracking software Ethovision 13 (Noldus, Leesburg, VA, US), the amount of time each mouse spent in the center or the periphery of the box was determined. The center (25 x 27.5 cm square around the

center of the box) and periphery (remainder of the box outside the center area) areas were predefined at the beginning of the experiment.

Novel Object Recognition

To determine whether SAH and/or MPO injection affects recognition memory, a novel object recognition test was performed on each group. Mice were placed in the open field box with the familiar object and given 30 minutes of exploration time. At the end of the 30 minutes, the novel object was introduced to the environment and mice were given an additional 5 minutes of exploration. Using Ethovision 13 software (Noldus, Leesburg, VA, US), mouse behavior was tracked, and the amount of time spent with each object was recorded.

Statistics

Graphpad Prism 7 (Graphpad, La Jolla,CA, US) software was used to analyze all of the data obtained. Student's t-test or analysis of variance (ANOVA) were used to determine whether differences between treatment groups were statistically significant.

Results

Localization of innate immune cells after subarachnoid hemorrhage.

As we have previously shown, neutrophils do not infiltrate the brain in significant numbers over the first three days after SAH compared to sham[5]. We therefore focused at the three-day timepoint on the meninges. Using flow cytometry, we found no significant difference in the total number of neutrophils in the meninges between the sham and SAH groups (Fig. 1A). Neutrophils are significantly increased three days after surgery in both sham and SAH groups, as

compared to mice at day 1 post surgery (Fig. 1A), which is not unexpected given that sham surgery disrupts tissue adjacent to the meninges. Importantly, by immunohistochemical analysis, neutrophils at day 1 and 3 show different patterns of distribution within the meninges. The majority of neutrophils in both groups are found within and adherent to the walls of the vasculature of the transverse sinus, but in the SAH group, increased neutrophils are seen in the outer tissues of the meninges (at both day 1 and 3 post hemorrhage) (Fig. 1B and C). Taken together, these data show that insults in or near the meninges leads to increased neutrophils near or in the vascular compartments in the meninges, but, in SAH, there is infiltration of neutrophils into the parenchyma of the meninges.

To determine whether the neutrophils observed in the meninges originate from the original hemorrhage or are entrained from the periphery, mice were injected intravenously with a FITC-conjugated anti-CD45 antibody 3 days post SAH. Thirty minutes after injection, mice were euthanized and their meninges were analyzed for neutrophil infiltration. Presence of CD45-FITC expressing neutrophils within the parenchyma of the meninges of SAH mice suggests active infiltration from the circulation (Fig. 1D). These results suggest that neutrophils actively enter the meninges during the critical period of inflammation from the circulation; they are not only from blood left over from the initial hemorrhage. This supports a coordinated, systemic inflammatory response that occurs between the brain hemorrhage and the onset of cerebral injury.

The loss of functional myeloperoxidase is protective in SAH

Three prominent neutrophil effector proteins, myeloperoxidase, elastase and NADPH oxidase, have been implicated in neuronal damage after ischemic stroke but have not been investigated in DCI after SAH [9,11,19]. Here, we analyzed the effects of these enzymes in the development of DCI after SAH. Using elastase KO, NADPH oxidase KO, and MPO KO mice, we characterized spatial memory function after SAH using the Barnes maze task. Of the three transgenic mice analyzed, only the MPO KO mouse was protected against the development of delayed spatial memory deficits (Fig. 2A). These results corroborate our previous finding of increased myeloperoxidase-dependent tyrosine modification (chloro-tyrosine) in the CSF of human patients three days after SAH, suggesting that MPO may be a critical player in the deficits observed after SAH in both mice and humans (Provencio *et al.*, 2010).

Immune cells in the CNS of the MPO KO mouse

To better understand why MPO-deficient mice do not develop DCI after SAH, we characterized the innate immune profile within the CNS of this mouse. Our WT results showed peak neutrophil infiltration occurring at day 3 post SAH (Fig. 1A-C). Therefore, our analysis of the MPO KO mouse was restricted to this time point. Similar to the WT control mouse, neutrophils were detected in the meninges of MPO KO mice (Fig. 2B.). In contrast to the WT data, the MPO KO mouse shows few neutrophils infiltrating to the meningeal parenchyma (Fig. 2C).

Both adaptive and innate immune cells populate the meninges of the normal mouse [20]. In order to investigate whether there are baseline differences in neutrophil numbers in the MPO KO mouse, flow cytometry was performed on the CNS of naïve MPO KO and WT mice. Interestingly, the MPO KO mouse have more $CD45^{+}$ cells in the brain and meninges than the

WT mouse (Supplemental Fig. 1A). The increased number of cells in the brain of the MPO KO mouse can be attributed to the high number of CD45 intermediate cells, microglia. Further analysis of brain and meninges separately showed that the brains of the MPO KO mice have considerably more microglia and monocytes than WT brains (Supplemental Fig. 1B). In the meninges, although MPO KO mice have more $CD45^{+}$ cells, they have fewer neutrophils and monocytes than WT mice (Supplemental Fig. 1C). Finally, although both mice have similar performance on the rotarod test, the naïve MPO KO mouse takes significantly longer to find the goal box in the Barnes maze tasks than the WT mouse (Supplemental Fig. 1D).

MPO KO mouse lacks spasm in the middle cerebral artery after SAH

A hallmark of DCI in SAH is the development of arterial vascular spasm (vasospasm). In the model used in this study, vasospasm is detected in the middle cerebral artery (MCA) 6 days after SAH[6]. Therefore, the MPO KO mouse was analyzed for the presence of vasospasm 6 days after SAH (Fig. 3A). The WT mouse showed increased constriction in the MCA 6 days after SAH (confirming our previous results), but no constriction was detected in the MPO KO mouse after SAH (Fig. 3A and B)[6]. This suggests that lack of MPO in the system decreases all of the manifestations of DCI, not just the spatial memory impairment.

SAH does not affect the level of reactive oxygen species (ROS) in the mouse hippocampus

The role of MPO in the production of ROS has been extensively studied in a number of disease models[21–23]. To investigate whether SAH leads to an increase level of ROS in the hippocampus, the level of lipid peroxidation was quantified using 4-hydroxynonenal (4-HNE). 4-HNE is generated as a result of oxidation of specific lipid groups in the membranes of cells,

including arachidonic and linoleic groups and is therefore a marker of ROS in tissue[24]. Our results show no significant change in the expression of 4-HNE in the CA1 region of the hippocampus in either the WT or the MPO KO mouse (Supplemental Fig. 2). This suggests that the oxidation level in the hippocampus does not appear to play a critical role in the development of DCI after SAH.

Biologically active MPO recapitulates the development of DCI in the MPO KO mouse after SAH

To determine the importance of the MPO enzyme in the development of DCI, we introduced biologically active MPO to the CSF of the MPO KO mouse at the time of SAH. The injection of MPO alone to the CSF of the MPO KO mouse at the time of the hemorrhage did not affect the animal's ability to find the escape hole in the Barnes maze task (Fig. 4B). Because superoxide ($O_2^{\cdot}$) is a substrate for MPO activity, as a control, H_2O_2 alone was introduced to the meninges of the MPO KO mouse. H_2O_2 alone did not show a difference (Fig. 4C). Conversely, MPO KO mice that were injected with both MPO and H_2O_2 in the CSF at the time of hemorrhage took three time as long to find the escape box most notably 8 days after SAH (Fig. 4D and E). Taken together, these results suggest that the lack of a functional MPO system including its oxidant partner is the basis for the absence of DCI in the MPO KO mouse.

An important question left unanswered is whether MPO is sufficient to cause the phenotype of DCI without SAH. To determine whether MPO alone is enough to cause cognitive deficits, biologically active MPO was added to the CSF of WT mice in the absence of a hemorrhage. Our results show that the addition of MPO, H_2O_2, and MPO^+ H_2O_2 to the CSF, in the absence of the

hemorrhage, is not enough to cause the deficit (Fig. 4F-H). This indicates that, although critical, MPO alone is not enough to cause DCI. Other, as yet unidentified, elements in the blood from the hemorrhage are necessary for the cognitive impairment observed after SAH.

Patients with SAH and DCI develop memory and executive function deficits but also report anxiety and mood disturbances[25]. To evaluate other domains of cognitive function, we investigated exploration behavior and anxiety in the WT and MPO KO mouse after the addition of MPO and H_2O_2. Both open field test and novel object recognition tasks showed no difference in any group (Supplemental Fig. 3). This supports the conclusion that the results of the Barnes Maze test were from spatial memory dysfunction, rather than freezing or lack of attention due to anxiety.

The MPO KO phenotype does not reduce Iba1$^+$ myeloid cell morphological changes associate with activation.

Insofar as neutrophils are not found within the hippocampus of the SAH mouse, we speculate that the action of neutrophils on neurons in the hippocampus requires a cell intermediate. SAH leads to changes in the composition of NMDA receptors at the postsynaptic cleft of the CA1 pyramidal neurons[5]. To investigate whether neutrophils interact with microglia, which, in turn, influence neuronal function, we characterized the effect of SAH on microglial morphology in the CA1 region of the hippocampus.

Microglia morphology was characterized using Iba1 expression in the hippocampus with the understanding that tissue macrophages will also express Iba1. Interestingly, no changes were

observed in the number of Iba1$^+$ cells or their intensity in the CA1 region of the WT and MPO KO mouse at either 3 or 6 days after SAH (data not shown). To determine whether the activation phenotype of these cells was affected after SAH, the number of cell processes was quantified using Scholl analysis. Though different from the amount of ramification observed in the naïve mouse (Supplemental Fig. 4), no significant changes were observed in the ramification of Iba1$^+$ cells between sham and SAH groups of the WT mouse at 3 days (Fig. 5B). Six days after SAH, Iba1$^+$ cells in the WT SAH mouse had significantly more processes than the sham mouse, suggesting a less activated state. On the other hand, Iba1$^+$ cells in the MPO KO mouse appear more complicated; on day 3, there is a trend for decreased ramification of Iba1$^+$ cells in the SAH group, however, by day 6, the ramification between sham and SAH groups are similar.

Astrocytes activation is decreased in MPO KO mice after SAH.

Astrocytes were characterized in the CA1 region of the hippocampus by their expression of GFAP and vimentin. In the WT, GFAP was abundantly expressed in the CA1 sub-region of the hippocampus at both day 3 (Fig. 6A) and day 6 (Fig. 6E). At day 3, although no changes were observed in the number of GFAP$^+$ astrocytes after SAH (Fig. 6C), GFAP intensity was significantly decreased in these cells (Fig. 6B). Furthermore, more astrocytes colocalized both GFAP and Vimentin 3 days after SAH (Fig. 6D), suggesting increased activation of these cells [26]. At day 6, both GFAP$^+$ cell number and intensity were significantly decreased after SAH (Figs. 6F and 6G) with no change in the colocalization of GFAP and vimentin (Fig. 6H). Interestingly, none of these changes were observed in the MPO KO mouse after SAH at either timepoints (Fig. 6A-E), suggesting these cells may be good candidates for intermediaries between the meninges and the brain.

Discussion

Neutrophil-mediated MPO is critical but not sufficient in the development of DCI after SAH.

Multiple models and methods of SAH in different species have been employed to investigate the underlying mechanism of vasospasm and DCI after subarachnoid hemorrhage[27–32]. By using a mild model of SAH without high-pressure injection of blood, arterial bleeding or aneurysm rupture, we are able to investigate the cognitive consequences of blood in cerebrospinal fluid independent of early brain injury and the initial circulatory arrest in the brain seen in more aggressive models. ROS production is increased and has been implicated in a number of models of SAH[33]. Interestingly, and contrary to findings in higher pressure SAH models, we observed no change in the level of ROS in our model despite development of DCI, suggesting that ROS levels are not the only cause of DCI[33]. This mild model of SAH provides the unique opportunity to understand how a CNS insult affects the brain without the confounding role of damaging pressure, thereby providing a tool to mechanistically dissect changes in cognition due to sterile immune interactions in the CNS.

The location of neutrophils after SAH raises questions about their function as modulators of neuronal dysfunction. We show that extravasation of neutrophils in the meninges affects spatial memory abnormalities, supporting our previous finding that late long-term potentiation in the hippocampus is impaired in a delayed fashion after SAH[5]. Neutrophil infiltration damages neurons in animal models of neurodegeneration and injury[1–4]. For example, the presence of neutrophils in the substantia nigra pars compacta has been implicated in the increased loss of

dopaminergic neurons in a $MPTP^+$ rodent model of Parkinson's Disease [2]. Following focal ischemia, neutrophil infiltration into the parenchyma coincides with the onset of neurological deficits[1]. In our model, the presence of neutrophils in the meningeal parenchyma and not infiltrating the brain proves detrimental after SAH suggesting an indirect effect on neuronal function either through their release of diffusible factors or activation of cell intermediaries. This same phenomenon occurs in mild brain contusions suggesting that neutrophil action from the meninges is a clinically important pathway that may not be restricted to SAH [34]. In fact, the stimulus to the CNS needed to elicit neutrophil responses appears to be mild as evidenced by increased neutrophil localization to the vasculature of the meninges in our sham surgery animals with no detectable behavioral defects.

Neutrophils contain primary and secondary granules with several enzymes critical to their antibacterial and inflammatory functions [8]. A few of these enzymes, NADPH oxidase [11], elastase [9] and MPO [19], have been implicated in neuronal damage/loss in models of ischemia and stroke. The present study shows that in SAH, only MPO plays a critical role in neuronal injury. In the Barnes maze task, MPO KO mice were not spared the initial effect of the hemorrhage. But unlike the WT, these mice did not develop the 'second injury' that leads to the development of DCI after SAH. Because the addition of MPO and its substrate, H_2O_2, reinstitutes the cognitive loss, we infer that MPO plays a critical role in delayed (i.e. secondary) injury to the CNS after SAH. Interestingly, the results of MPO administration to WT mice shows that MPO by itself is not enough; some component(s) from the initial hemorrhage are needed in the meninges to cause cognitive defects.

In light of these results, the question arises as to whether the breakdown components of the hemorrhage have a direct effect on the activity of the MPO enzyme or, whether the combination of damage from the hemorrhage and the action of neutrophils from MPO work synergistically to lead to brain damage. MPO's known function is to produce the ROS HOCl and peroxinitrite. MPO alone was unable to recapitulate the memory dysfunction in the MPO KO mouse without the action of peroxide suggesting that ROS may be produced in the meninges. Peroxide injection alone in the meninges was not sufficient to cause the spatial memory deficits suggesting that this is not a nonspecific effect of ROS production. However, there are no changes in our measures of ROS in the CA1 region suggesting the final pathway to neuronal dysfunction is not through ROS in the hippocampus.

A number of inflammatory triggers from blood products have been investigated in SAH. Biliverdin and bilirubin oxidation products (BOXes), breakdown products of hemoglobin, have been implicated in vessel damage after hemorrhage in the CNS [35,36]. Ferrous ion, Fe^{2+}, also a breakdown product of hemoglobin, in the presence of peroxide, H_2O_2, is implicated with neuronal damage after endothelial cell loss and blood-brain barrier breakdown [37–39]. MPO like other peroxidases is a heme enzyme, its catalytic domain contains a ferric iron which acts as an oxidant in both the halogenation and peroxidase cycle of the enzyme[22]. Our lab has previously demonstrated an increased level of free iron in the CSF of SAH patients. Indeed, there is a negative correlation between the occurrence of DCI and the expression of the iron metabolic enzyme ceruloplasmin suggesting that disruption of iron homeostasis in the brain can be detrimental to neuronal function [40]. From these findings, one can suspect that the excess of ferrous iron after SAH may influence the activity of MPO. Recent studies have demonstrated

that through the production of hypochlorous acid, MPO inhibits its own activity by the release of its ferric iron [41]. It is therefore plausible that in our model, MPO activity leads to increase free iron in the system, which is known to be toxic to neurons. Further studies to investigate the role of free iron associate with MPO are warranted.

Astrocytes are the most likely cell intermediate between neutrophils and neurons.

The restriction of neutrophils to the meningeal space in our model suggests an indirect effect on neurons, likely through its action on glial cells. In the present study, we focused on the possibility of astrocytes or microglia being the intermediate cell between the meningeal space and the brain parenchyma. Since MPO KO mice do not develop DCI after SAH, our analysis was focused on finding a cell that exhibited changes in the WT and not in the MPO KO mouse. In this study, we focused on the hippocampus as the behavioral changes on the Barnes maze test localize to that area of the brain and we have previously described impaired late long-term potentiation (L-LTP) in the hippocampus in this model[6].

The question of which cell intermediary plays a role in the development of memory dysfunction is critical to understanding the mechanism of neutrophil (i.e. MPO) action. The two most intriguing choices are microglia and astrocytes as they both have the propensity to react to inflammatory signals[42].

Microglia show very little change after SAH in our model, making them unlikely to be the cell intermediary between neutrophils in the meninges and hippocampal neurons. In a previous study[5], we reported that the microglia in the dorsal hippocampus were more ameboid

(appeared more activated) in SAH than sham. The present project focused on changes within the CA1 subregion alone. Analysis of the ramification, activation profile after SAH, in both genotypes yielded unexpected results. Three days after SAH, the WT showed no change in the number of processes observed in microglia across treatment groups. However, 6 days after SAH the WT SAH mouse showed more ramification than the sham mouse. This would indicate that microglia cells are only transiently affected by the hemorrhage. On the other hand, in the MPO KO mouse no significant changes were observed in either group at each timepoint, although at day 3, a trend of more activation was observed in the MPO KO SAH mouse. Taken with the previous data, it would appear that the delayed activation seen in the dorsal hippocampus is not apparent in the area of the brain where we would expect memory dysfunction is focused [5]. This suggests that microglia are less likely to be the intermediary cell between neutrophils and neurons. We cannot rule out that microglial activation in other parts of the hippocampal formation may have distal effects on cognition.

Conversely, the changes induced in astrocytes by SAH were abolished by the absence of functional MPO, suggesting that the astrocytes are a better candidate intermediary cell through which meningeal neutrophils affect neuronal function in the brain parenchyma. Astrocytes show decreased cell numbers and expression of critical cytoskeletal protein in the WT after SAH; changes abolished in the MPO KO mouse. Astrocytes are critical to the maintenance of homeostatic balance between the nervous, immune, and circulatory systems under normal conditions. Their ability to support neurons, through the provision of neurotransmitters, lactate, etc., is critical to the maintenance of normal neuronal function in the CNS[43]. Astrocytes have been shown to play a critical role in neuroinflammation. For example, astrocytes modulate

microglial expression and release of the proinflammatory cytokine interleukin 12 *in vitro* [44]. Furthermore, the physical barrier produced by astrocytes is critical in modulating the interaction of injured areas with the immune system in animal models of multiple sclerosis and traumatic brain injury [45,46]. In our model, signs of impaired function, particularly decreased GFAP expression and death after SAH, may hinder their ability to 'protect' neurons from an inflammatory insult within the meninges. Indeed, knocking out GFAP has been associated with poor outcomes in animal models of infection in the CNS[47]. It is important to note that the mechanism through which astrocytes are lost in our system is yet unknown. Therefore, more experimentation needs to be conducted to better understand how they are affected in our system.

Conclusions

Because, among mature immune cells, only neutrophils express MPO, our data support the conclusion that neutrophils influence neuronal function in SAH without infiltrating the brain parenchyma (consistent with our previous data). MPO is critical to the cognitive changes observed in SAH mice. The role of MPO in modulating cognitive changes is complicated: MPO is not sufficient to cause cognitive deficits in WT mice without SAH, and hemorrhage without MPO does not lead to deficits. But, with blood in the CSF space, MPO and H_2O_2 recapitulate cognitive deficits in MPO KO mice. Taken together, these results suggest that either MPO and/or blood breakdown product can theoretically be targeted to mitigate the development of DCI after SAH.

Therefore, an important next step is to determine whether small molecule inhibition of MPO can be used therapeutically to mitigate the development of DCI after SAH. A recent study

demonstrated that inhibition of MPO increased ventricular function in a mouse model of myocardial infarction [48]. Such an approach holds promise for the prevention or treatment of DCI after SAH.

Abbreviations

CNS: central nervous system; **NADPH**: nicotinamide adenine dinucleotide phosphate; **CST:** cerebrospinal fluid; **SAH:** subarachnoid hemorrhage; **DCI:** delayed cerebral injury; **CD11/CD18a**: cluster of differentiation 11 and 18a, alpha integrin; **MPO:** myeloperoxidase; **KO:** knockout out or deficient; **WT:** wildtype; **HOCL:** hypochlorous acid; **H_2O_2:** hydrogen peroxide; **PBS:** phosphate buffer saline; **BSA:** bovine serum albumin; **CD45:** Cluster of differentiation 45, common leukocyte marker; **Ly6G:** lymphocyte antigen 6 complex G; **Ly6C:** lymphocyte antigen 6 complex C; **DMEM:** Dulbecco's modified eagle medium; **Ly6B:** lymphocyte antigen 6 complex B; **4-HNE:** 4-hydroxynonenal; **DAPI:** 4,6-diamino-2-phenylindole; **GFAP:** glial fibrillary acidic protein; **Iba1:** ionized calcium binding adaptor molecule 1; **CA1:** Cornu Ammonis area 1; **NT:** neutrophil; **MCA:** middle cerebral artery; **ROS:** reactive oxygen species; **MPTP:** 1-methyl-4-phenyl-1,2,3,6-tetrahydropyridine; **BOXes:** biliverdin and bilirubin oxidation products; **L-LTP:** late long-term potentiation.

Declarations

Ethics approval and Consent to participate: All animal experiments were approved by the Institutional Animal Care and Use Committee at the University of Virginia. No human participated in the presented study.

Consent for publication: NA

Availability of data and materials: NA

Competing interests: JJP has a grant support from Minnetronix, Inc. to study the role inflammation after SAH. The other authors of this paper, APC, PP, WG, and DT declare that they have no competing interests.

Funding: This study was supported by grant NIH NS074997 awarded to Dr. JJ Provencio.

Author contributions: JJP conceived of the study and supervised the design and performance of the experiments. APC contributed to the research design and performed the majority of the experiments and data analysis presented. APC also wrote the manuscript under the guidance and supervision of JJP. PP contributed the original research design of the concept presented in this paper, performed and analyzed the foundational experiments using the transgenic mice presented in the paper, and help in review and revision of the manuscript. WG performed the microglia Scholl analysis experiments, including staining and data analyses, and participated in review and revision of the manuscript. DT conducted the behavioral experiments presented in the supplemental figure 1, and participated in review and revision of the manuscript.

Acknowledgments: The authors would like to extend their gratitude to Dr. Kipnis' lab for all their help with the study, including Igor Smirnov for surgery assistance, Antoine Louveau for microscopy, and Jasmin Hertz for Flow cytometry. Further thanks from Elizabeth Frost (Dr. Lukens' lab) for further help with flow cytometry analysis. Many thanks to the Brain Immunology and Glia (BIG) center at UVA for all the equipment made available to us to complete this project. Thanks to Drs. John R. Lukens and Kevin S. Lee for review of the manuscript.

References

1. Barone F.C. Hillegass, LM. Price, WJ. White, RF. Lee, EV. Feuerstein, GZ. Sarau, HM. Clark, RK. Griswold,DE. Polymorphonuclear leukocyte infiltration into cerebral focal ischemic. EmbaseJournal Neurosci Res. 1991;345:336–45.
2. Ji K-A, Eu MY, Kang S-H, Gwag BJ, Jou I, Joe E-H. Differential neutrophil infiltration contributes to regional differences in brain inflammation in the substantia nigra pars compacta and cortex. Glia. 2008;56:1039–47.
3. Shultz SR, Bao F, Weaver LC, Cain DP, Brown A. Treatment with an anti-CD11d integrin antibody reduces neuroinflammation and improves outcome in a rat model of repeated concussion. J Neuroinflammation. Journal of Neuroinflammation; 2013;10:1. Available from: Journal of Neuroinflammation
4. Herz J, Sabellek P, Lane TE, Gunzer M, Hermann DM, Doeppner TR. Role of neutrophils in exacerbation of brain injury after focal cerebral ischemia in hyperlipidemic mice. Stroke. 2015;46:2916–25.
5. Provencio JJ, Swank V, Lu H, Brunet S, Baltan S, Khapre R V., et al. Neutrophil depletion after subarachnoid hemorrhage improves memory via NMDA receptors. Brain Behav Immun. Elsevier Inc.; 2016;54:233–42.
6. Provencio JJ, Altay T, Smithason S, Moore SK, Ransohoff RM. Depletion of Ly6G/C^{+} cells ameliorates delayed cerebral vasospasm in subarachnoid hemorrhage. J Neuroimmunol. Elsevier B.V.; 2011;232:94–100.
7. Amulic B, Cazalet C, Hayes GL, Metzler KD, Zychlinsky A. Neutrophil Function: From Mechanisms to Disease. Annu Rev Immunol. 2012;30:459–89.
8. Kolaczkowska E, Kubes P. Neutrophil recruitment and function in health and inflammation. Nat Rev Immunol . Nature Publishing Group; 2013;13:159–75.
9. Matayoshi H, Hirata T, Yamashita S, Ishida K, Mizukami Y, Gondo T, et al. Neutrophil elastase inhibitor attenuates hippocampal neuronal damage after transient forebrain ischemia in rats. Brain Res . Elsevier B.V.; 2009;1259:98–106.
10. Yu G, Liang Y, Zheng S, Zhang H. Inhibition of Myeloperoxidase by N-Acetyl Lysyltyrosylcysteine Amide Reduces Oxidative Stress-Mediated Inflammation, Neuronal Damage, and Neural Stem Cell Injury in a Murine Model of Stroke. J Pharmacol Exp Ther . 2018;364:311–22.
11. Chen G, Ye X, Zhang J, Tang T, Li L, Lu P, et al. Limb remote ischemic postconditioning reduces ischemia-reperfusion injury by inhibiting NADPH oxidase activation and MYD88-TRAF6-P38MAP-kinase pathway of neutrophils. Int J Mol Sci. 2016;17.
12. Ma MW, Wang J, Dhandapani KM, Brann DW. Deletion of NADPH oxidase 4 reduces severity of traumatic brain injury. Free Radic Biol Med. Elsevier B.V.; 2018;117:66–75.
13. Tonai T, Shiba KI, Taketani Y, Ohmoto Y, Murata K, Muraguchi M, et al. A neutrophil elastase inhibitor (ONO-5046) reduces neurologic damage after spinal cord injury in rats. J Neurochem. 2001;78:1064–72.
14. Provencio JJ, Fu X, Siu A, Rasmussen PA, Hazen SL, Ransohoff RM. CSF neutrophils are implicated in the development of vasospasm in subarachnoid hemorrhage. Neurocrit Care . 2010;12:244–51.
15. Schneider UC, Schiffler J, Hakiy N, Horn P, Vajkoczy P. Functional analysis of Pro-inflammatory properties within the cerebrospinal fluid after subarachnoid hemorrhage in vivo and in vitro. J Neuroinflammation. 2012;9:1–10.
16. Altay T, Smithason S, Volokh N, Rasmussen PA, Ransohoff RM, Provencio JJ. A novel method for subarachnoid hemorrhage to induce vasospasm in mice. J Neurosci Methods.

2009;183:136–40.
17. Gadani SP, Smirnov I, Smith AT, Overall CC, Kipnis J. Characterization of meningeal type 2 innate lymphocytes and their response to CNS injury. J Exp Med . 2017;214:285–96.
18. Derecki N, Norris G, Derecki N, Kipnis J. Microglial Sholl Analysis. Protoc Exch . 2014.
19. Yu G, Liang Y, Huang Z, Jones DW, Pritchard KA, Zhang H. Inhibition of myeloperoxidase oxidant production by N-acetyl lysyltyrosylcysteine amide reduces brain damage in a murine model of stroke. J Neuroinflammation . Journal of Neuroinflammation; 2016;13:1–13.
20. Mrdjen D, Pavlovic A, Hartmann FJ, Schreiner B, Utz SG, Leung BP, et al. High-Dimensional Single-Cell Mapping of Central Nervous System Immune Cells Reveals Distinct Myeloid Subsets in Health, Aging, and Disease. Immunity . Elsevier Inc.; 2018;48:380–395.e6.
21. van der Veen BS, de Winther MP, Heeringa P. Myeloperoxidase: molecular mechanisms of action and their relevance to human health and disease. Antioxidants Redox Signal . 2009;11:2899–937.
22. Davies MJ. Myeloperoxidase-derived oxidation: mechanisms of biological damage and its prevention. J Clin Biochem Nutr . 2011;48:8–19.
23. Ray RS, Katyal A. Neuroscience and Biobehavioral Reviews Myeloperoxidase : Bridging the gap in neurodegeneration. Neurosci Biobehav Rev. Elsevier Ltd; 2016;68:611–20.
24. Zhong H, Yin H. Role of lipid peroxidation derived 4-hydroxynonenal (4-HNE) in cancer: focusing on mitochondria. Redox Biol . 2015;4:193–9.
25. Al-Khindi T, MacDonald RL, Schweizer TA. Cognitive and functional outcome after aneurysmal subarachnoid hemorrhage. Stroke. 2010;41.
26. Janeczko K. Co-expression of GFAP and vimentin in astrocytes proliferating in response to injury in the mouse cerebral hemisphere. A combined autoradiographic and double immunocytochemical study. Int J Dev Neurosci . 1993;11:139–47.
27. Bühler D, Schüller K, Plesnila N. Protocol for the Induction of Subarachnoid Hemorrhage in Mice by Perforation of the Circle of Willis with an Endovascular Filament. Transl Stroke Res. 2014;5:653–9.
28. Pluta RM, Bacher J, Skopets B, Hoffmann V. A non-human primate model of aneurismal subarachnoid hemorrhage (SAH). Transl Stroke Res . 2014;5:681–91.
29. Sehba FA. Rat endovascular perforation model. Transl Stroke Res . 2014;5:660–8.
30. Güresir E, Schuss P, Borger V, Vatter H. Rat cisterna magna double-injection model of subarachnoid hemorrhage - background, advantages/limitations, technical considerations, modifications, and outcome measures. Acta Neurochir Suppl . 2015;120:325–9.
31. Kikkawa Y, Kurogi R, Sasaki T. The single and double blood injection rabbit subarachnoid hemorrhage model. Transl Stroke Res . 2015;6:88–97.
32. Marbacher S, Fathi AR, Muroi C, Coluccia D, Andereggen L, Neuschmelting V, et al. The rabbit blood shunt subarachnoid haemorrhage model. Acta Neurochir Suppl . 2015;120:337–42.
33. Ayer RE, Zhang JH. Oxidative stress in subarachnoid haemorrhage: Significance in acute brain injury and vasospasm. Acta Neurochir Suppl. 2008;33–41.
34. Roth TL, Nayak D, Atanasijevic T, Koretsky AP, Latour LL, McGavern DB. Transcranial amelioration of inflammation and cell death after brain injury. Nature . 2014;505:223–8.
35. Clark JF, Loftspring M, Wurster WL, Beiler S, Beiler C, Wagner KR, et al. Bilirubin oxidation products, oxidative stress, and intracerebral hemorrhage. Acta Neurochir Suppl . 2008;105:7–12.
36. Clark JF, Harm A, Saffire A, Biehle SJ, Lu A, Pyne-Geithman GJ. Bilirubin oxidation

products seen post subarachnoid hemorrhage have greater effects on aged rat brain compared to young. Acta Neurochir Suppl . 2011;110:157–62.
37. Bhasin RR, Xi G, Hua Y, Keep RF, Hoff JT. Experimental intracerebral hemorrhage: effect of lysed erythrocytes on brain edema and blood-brain barrier permeability. Acta Neurochir Suppl . 2002;81:249–51.
38. Chang EF, Claus CP, Vreman HJ, Wong RJ, Noble-Haeusslein LJ. Heme regulation in traumatic brain injury: Relevance to the adult and developing brain. J Cereb Blood Flow Metab. 2005;25:1401–17.
39. Lok J, Leung W, Murphy S, Butler W, Noviski N, Lo EH. Intracranial hemorrhage: mechanisms of secondary brain injury. Acta Neurochir Suppl . 2011;111:63–9.
40. Gomes JA, Selim M, Cotleur A, Hussain MS, Toth G, Koffman L, et al. Brain iron metabolism and brain injury following subarachnoid hemorrhage: iCeFISH-pilot (CSF iron in SAH). Neurocrit Care . 2014;21:285–93.
41. Maitra D, Shaeib F, Abdulhamid I, Abdulridha RM, Saed GM, Diamond MP, et al. Myeloperoxidase acts as a source of free iron during steady-state catalysis by a feedback inhibitory pathway. Free Radic Biol Med . Elsevier; 2013;63:90–8.
42. Stoll G, Jander S, Schroeter M. Inflammation and glial responses in ischemic brain lesions. Prog Neurobiol. 1998;56:149–71.
43. Cekanaviciute E, Buckwalter MS. Astrocytes: Integrative Regulators of Neuroinflammation in Stroke and Other Neurological Diseases. Neurotherapeutics . Neurotherapeutics; 2016;13:685–701.
44. Aloisi F, Penna G, Cerase J, Menéndez Iglesias B, Adorini L. IL-12 production by central nervous system microglia is inhibited by astrocytes. J Immunol (Baltimore, Md 1950) . 1997;159:1604–12.
45. Voskuhl RR, Peterson RS, Song B, Ao Y, Morales LBJ, Tiwari-Woodruff S, et al. Reactive Astrocytes Form Scar-Like Perivascular Barriers to Leukocytes during Adaptive Immune Inflammation of the CNS. J Neurosci . 2009;29:11511–22.
46. Bush TG, Puvanachandra N, Horner CH, Polito A, Ostenfeld T, Svendsen CN, et al. Leukocyte infiltration, neuronal degeneration, and neurite outgrowth after ablation of scar-forming, reactive astrocytes in adult transgenic mice. Neuron. 1999;23:297–308.
47. Stenzel W, Soltek S, Schluter D, Deckert M. The intermediate filament GFAP is important for the control of S. aureus induced brain abscess and toxoplasma encephalitis. Acta Neuropathol. 2004;108:367.
48. Ali M, Pulli B, Courties G, Tricot B, Sebas M, Iwamoto Y, et al. Myeloperoxidase Inhibition Improves Ventricular Function and Remodeling After Experimental Myocardial Infarction. JACC Basic to Transl Sci. 2016;1:633–43.

Figure legends

Figure 1: Neutrophils extravasate into the meninges after SAH. (**A**) Neutrophils ($CD11B^{+}Ly6G^{+}$) are found in the meninges of both sham and SAH mice. Representative flow cytometry plots of neutrophils 1 and 3 days post SAH/Sham (left). Although the $CD11B^{+}Ly6G^{+}$ population showed no significant difference between sham and SAH groups at each time point, more neutrophils were observed in the

meninges 3 days after surgery when compared to the naïve and 1 day groups (Two way ANOVA: % of CD11B population $p<0.001$; $F(1,15)= 46.95$; number of $Ly6G^+$ cell $p<0.001$ $F(1,27)= 27.81$). (**B**) Confocal micrographs showing the presence of neutrophils (red; NT 7/4) in two locations within the meninges, around the vasculature of the transverse sinus and in the meningeal parenchyma. One day after surgery, in both sham and SAH mice, the majority of neutrophils are located in or around the transverse sinus. 3 days after surgery, neutrophils remain in the proximity of the transverse sinus in both groups, but significantly more cellular infiltration is observed in the parenchyma of the meninges of the SAH mouse when compared to the sham (quantified in **C**). Scale bar = 50 µm. (**D**) 3 days after SAH, anti-CD45 antibody administered intravenously 30 minutes prior to tissue fixation reveals continuing infiltration of peripheral neutrophils (white arrows) into the meninges after the hemorrhage suggesting continued recruitment of neutrophils after the initial insult, n=3.

Figure 2: Myeloperoxidase KO (MPO KO) mice do not develop memory deficits after SAH. (**A**) Escape latency of mice lacking functional elastase, NADPH oxidase, and myeloperoxidase (MPO) were tested for 7 days starting on the 3rd day after surgery in the Barnes Maze spatial memory task. Of the three transgenic mice characterized, only MPO deficient (MPO KO) mice do not develop the delayed deficits associated with the task after SAH (boxed area). We therefore characterized the MPO KO mouse further. (**B**) Neutrophils are observed in the meninges of both sham and SAH MPO KO mice (Student's t-test; $p<0.05$) (**C**) Unlike the WT mouse (shown from figure 1B), very few neutrophils are found in the meningeal parenchyma of the MPO KO mouse 3 days after surgery. Quantification shows that the number of neutrophils observed in the meninges is the same between the MPO KO sham and SAH mice 3 days after surgery. Scale bar = 50 µm.

Figure 3: Myeloperoxidase null mouse lacks vasospasm in the middle cerebral artery after subarachnoid hemorrhage (SAH). (**A**) (Left) Example of site of measurements for the determination of vasospasm (left). MCA= middle cerebral artery, ACA= anterior cerebral artery, PCom= posterior

cerebral artery. Red arrow points to measurement point. (Right) Representative micrographs of middle cerebral artery segments of WT and MPO KO mice at the time of peak vasospasm (6 days after SAH) showing constriction of the MCA in SAH (red arrow) but not in sham or SAH in MPO KO mice. Scale bar = 500μm. White lines denote location of vessel walls without constriction. (**B**) WT mice show a significant decrease in vessel diameter 6 days after SAH (Student's t-test; p=0.038). No significant change in vessel diameter was observed in the MPO KO mice.

Figure 4: Biologically active MPO recapitulates delayed cognitive deficits in the MPO KO mouse after SAH. Biologically active MPO and H_2O_2 were injected into the CSF at the time of hemorrhage in the MPO KO mouse. On Barnes maze test: (**A**) As previously shown, MPO KO mice did not develop delayed cognitive deficits after SAH. (**B and C**) Neither the introduction of exogenous MPO alone nor H_2O_2 alone in the cerebrospinal fluid (CSF) of the MPO KO mouse during SAH was sufficient to significantly affect the latency to find the goal box. (**D**) The addition of MPO and H_2O_2 together does recapitulate the late cognitive deficit observed in the wildtype mouse. (**E**) A focused analysis on day 8 after surgery shows a significant increase in latency to escape between the MPO KO sham and the MPO KO mouse with MPO and H_2O_2 (Student's t-test; p=0.028). Biologically active MPO and H_2O_2 are injected into the CSF at of the sham WT mouse at the time of surgery. (**F-H**) The addition of MPO, H_2O_2, MPO and H_2O_2 to the CSF of the wildtype (B6) sham mice does not lead to delayed cognitive deficits.

Figure 5: Iba1$^+$ myeloid cells (microglia and tissue macrophages) in the CA1 region of the hippocampus do not appear activated after SAH in both WT and MPO KO mice. (**A**) Representative confocal micrographs depicting the morphology and density of Iba1$^+$ cells (green) in sham and SAH mice 3- and 6-days post-surgery. Scale bar = 50 μm. (**B**) Scholl analysis of the activation status of Iba1$^+$ cells (cells have fewer processes when more activated) of both sham and SAH mice. 3 days after surgery, similar number of processes was observed on Iba1$^+$ cells of the B6 SAH and sham mice (Two-way ANOVA; p=0.119). By day 6, there is more ramification of the SAH mice suggesting the Iba1$^+$ cells are

less activated (Two-way ANOVA; p=0.004). In the MPO KO mice, SAH leads to a trend towards fewer ramifications (p=0.058). There were no changes in the number of processes observed in MPO KO mouse 6 days after SAH when compared to the MPO KO sham group (Two-way ANOVA; p=0.897).

Figure 6: Dynamic changes in astrocytes cytoskeletal protein expression in the wildtype after SAH is absent in the MPO KO mouse. (**A, E**) Representative confocal micrographs of GFAP (red) and Vimentin (green) expressing astrocytes in the CA1 subregion of the hippocampus 3- and 6-days post-surgery. Scale bar= 50µm. (**B**) 3 days after surgery, a significant decrease in GFAP intensity was observed in the SAH WT mouse (Student's t-test; p=0.047). No changes were observed in GFAP intensity in the MPO KO mouse. (**C**) SAH had no effect on the number of astrocytes at this time point. (**D**) There was a significantly increased colocalization of GFAP and vimentin in the wildtype mouse (Student's t-test; p=0.005). No change was observed in the colocalization of the two proteins in the MPO KO mouse after SAH. (**F, G**) Six days after surgery, both the number of $GFAP^+$ cells and GFAP intensity were significantly decreased in the wildtype mouse after SAH (Student's t-test; p=0.004 and p=0.006 respectively). (**H**) No changes were observed in the colocalization of GFAP and vimentin at this time point in either group.

Supplementary figure legends

Supplemental figure 1: Immunological characterization of the CNS compartment of the naïve wildtype and MPO KO mouse. (**A**) The naïve MPO KO mouse (n=5) contains more immune cells in both the meninges and brain parenchyma when compared to the wildtype mouse (n=5). Specifically, significantly more microglia were found in the brain of the MPO KO mouse. (**B**) More immune cells, specifically monocytes, are present in the brain of the naïve MPO KO mouse than that of the wildtype. (**C**) In the meninges, the number of monocytes and neutrophils is considerably lower in the MPO KO brain when compared to the wildtype control brain. (**D**) To determine whether behavioral baseline

differed across the two genotypes both Barnes maze and rotarod tasks were performed. At baseline, both genotypes performed similarly on the rotarod task. However, the MPO KO naïve mouse takes longer to enter the escape hole in the Barnes maze task.

Supplemental figure 2: SAH does not affect the level of lipid peroxidation in the CA1 subregion of the hippocampus. (**A**) Representative confocal micrographs of 4-HNE (lipid peroxidation) in the CA1 region after surgery. (**B**) No significant difference (One -way ANOVA; $p<0.05$) was observed in the expression of 4-HNE in the CA1 region of the wildtype and MPO KO mouse 3 days after SAH.

Supplemental figure 3: Addition of biologically active MPO to the CSF of mice has no effect on mice exploratory behavior. (**A, B**) The injection of MPO to the CSF of both wildtype and MPO KO mice does not impede the ability to explore a novel environment. (**C, D**) Nor does it affect the animal curiosity towards a novel object. There is a trend that MPO mice administered MPO enzyme regard the novel object less often than MPO mice without MPO added.

Supplemental figure 4: Morphology of naïve iba1 positive cells in the hippocampus. (**A**) Representative confocal micrograph of $Iba1^+$ cells in the hippocampus. Scale bar = 100 μm. (**B**) gray scale image is a representative image of the morphology of an $Iba1^+$ cells in the hippocampus. Graph represents the average number of ramifications found on an $Iba1^+$ cells. Each point represents the average counts from 3 different mice. In each mouse, 3-6 individual cells were randomly chosen and analyzed.

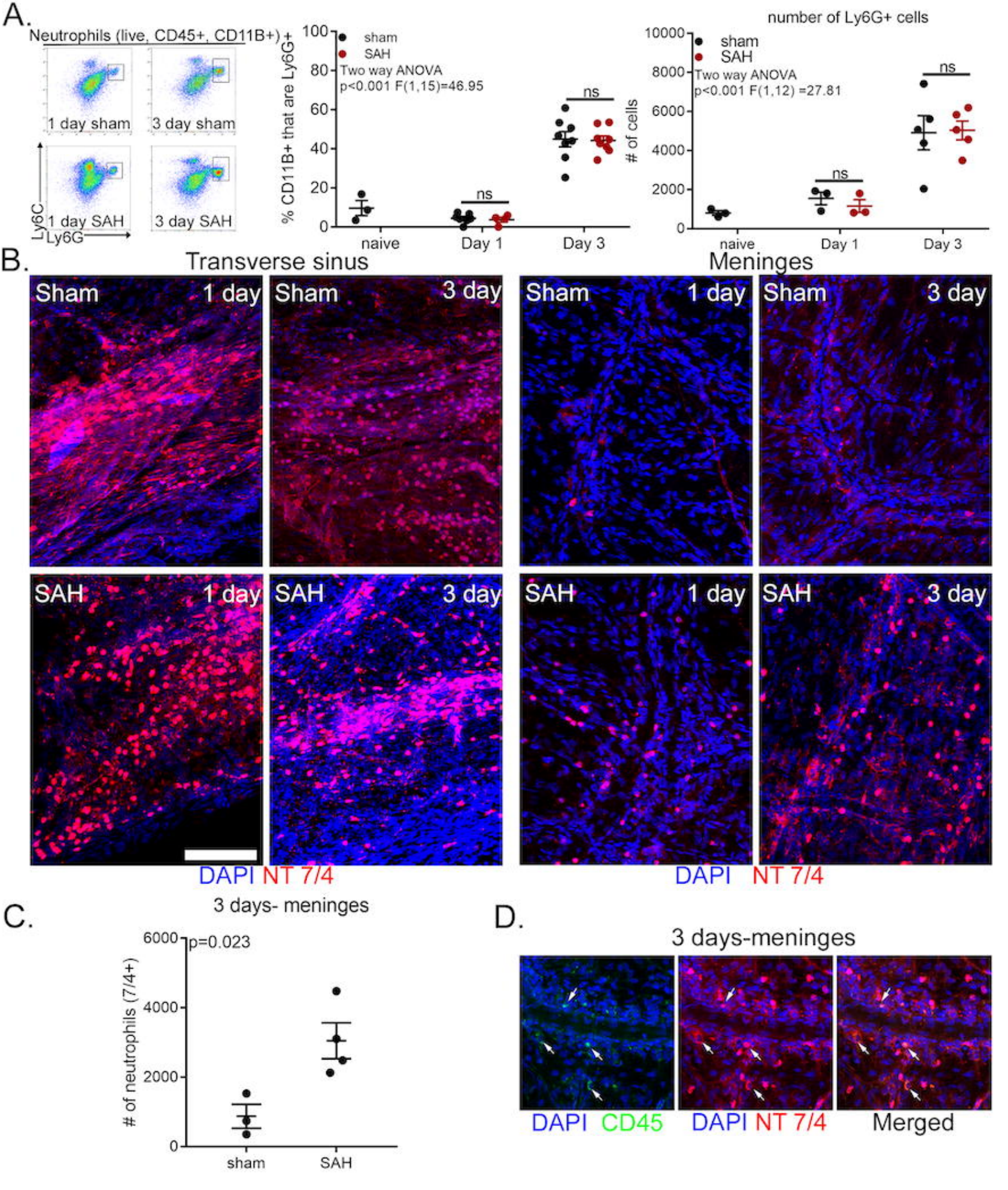
A.
Neutrophils (live, CD45+, CD11B+)
1 day sham
3 day sham
1 day SAH
3 day SAH
Ly6C
Ly6G
% CD11B+ that are Ly6G+
sham
SAH
Two way ANOVA
p<0.001 F(1,15)=46.95
ns
naive
Day 1
Day 3
number of Ly6G+ cells
# of cells
Two way ANOVA
p<0.001 F(1,12) =27.81
B.
Transverse sinus
Meninges
Sham
SAH
1 day
3 day
DAPI NT 7/4
C.
3 days- meninges
# of neutrophils (7/4+)
p=0.023
D.
3 days-meninges
DAPI CD45
DAPI NT 7/4
Merged

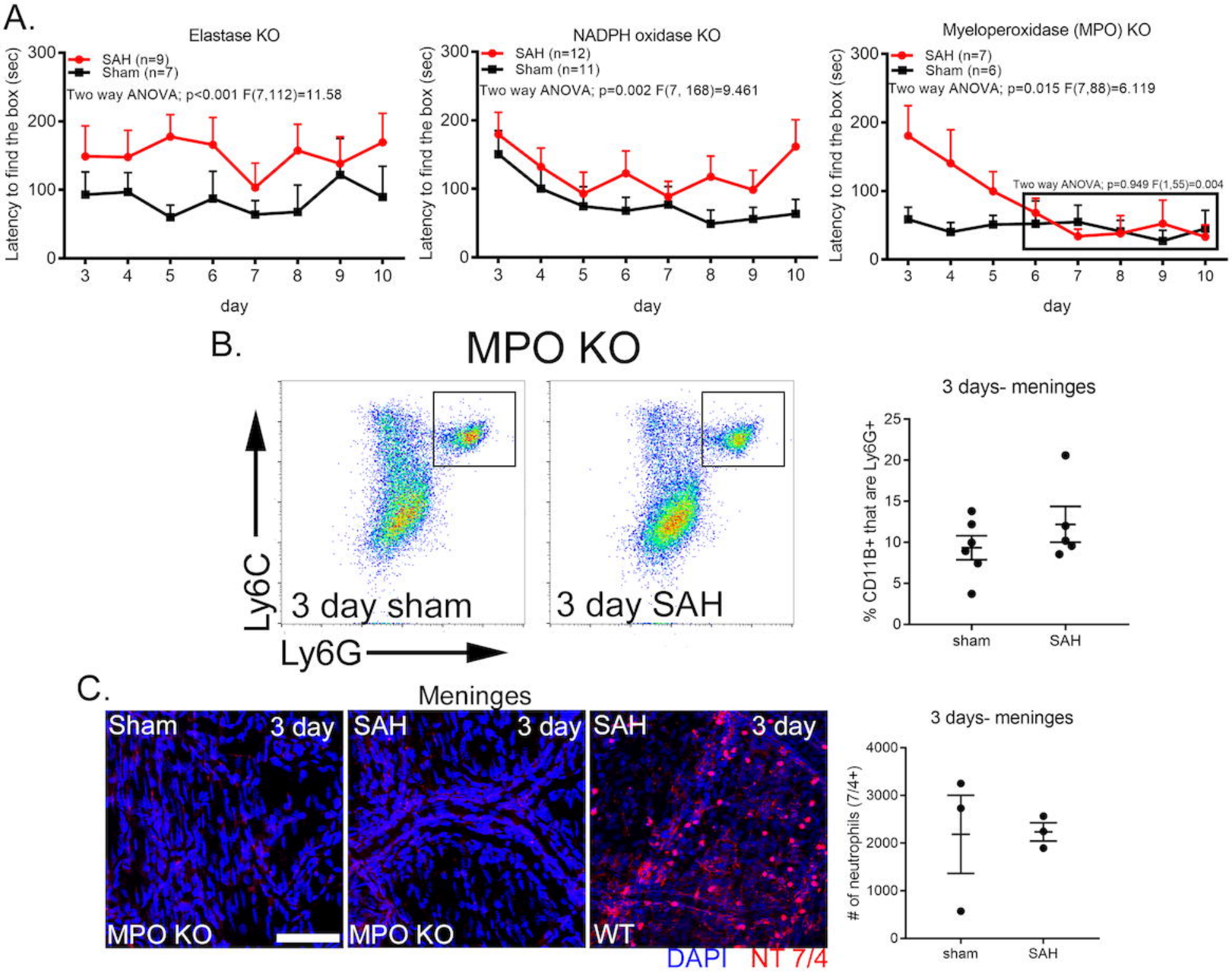
A.
Elastase KO
SAH (n=9)
Sham (n=7)
Two way ANOVA; p<0.001 F(7,112)=11.58
Latency to find the box (sec)
day
NADPH oxidase KO
SAH (n=12)
Sham (n=11)
Two way ANOVA; p=0.002 F(7, 168)=9.461
Myeloperoxidase (MPO) KO
SAH (n=7)
Sham (n=6)
Two way ANOVA; p=0.015 F(7,88)=6.119
Two way ANOVA; p=0.949 F(1,55)=0.004
B.
MPO KO
3 day sham
3 day SAH
Ly6C
Ly6G
3 days- meninges
% CD11B+ that are Ly6G+
sham
SAH
C.
Meninges
Sham 3 day
SAH 3 day
SAH 3 day
MPO KO
MPO KO
WT
DAPI NT 7/4
3 days- meninges
# of neutrophils (7/4+)
sham
SAH

A.

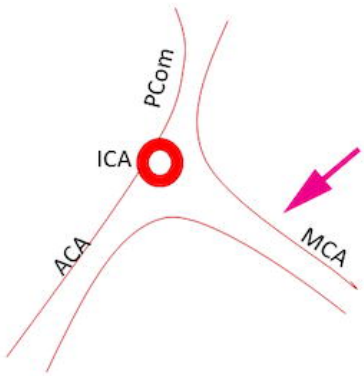
PCom
ICA
ACA
MCA

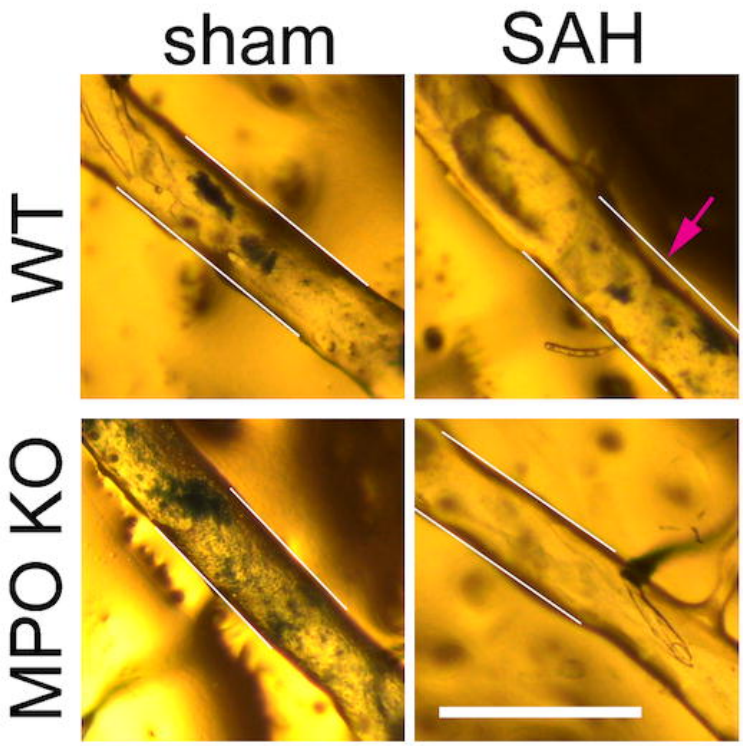
sham
SAH
WT
MPO KO

B.

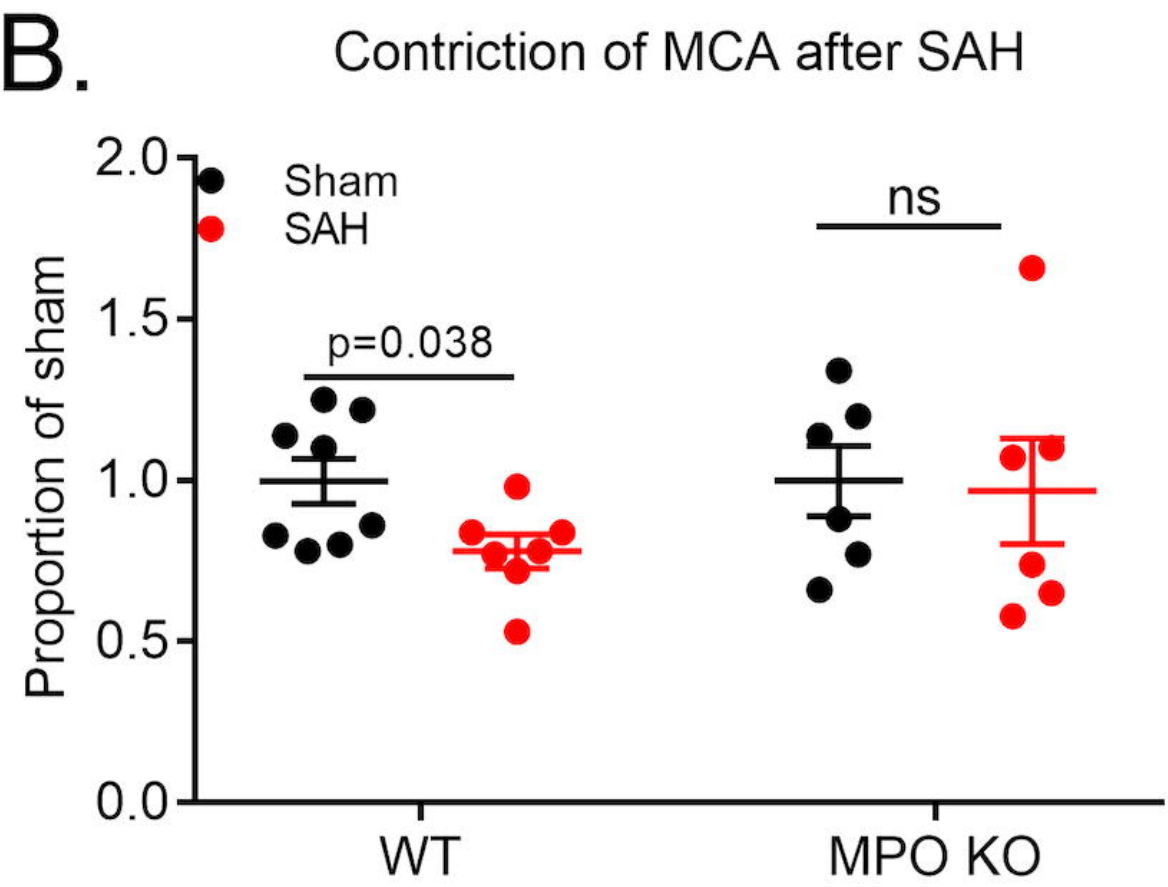
Contriction of MCA after SAH
Proportion of sham
2.0
1.5
1.0
0.5
0.0
Sham
SAH
p=0.038
ns
WT
MPO KO

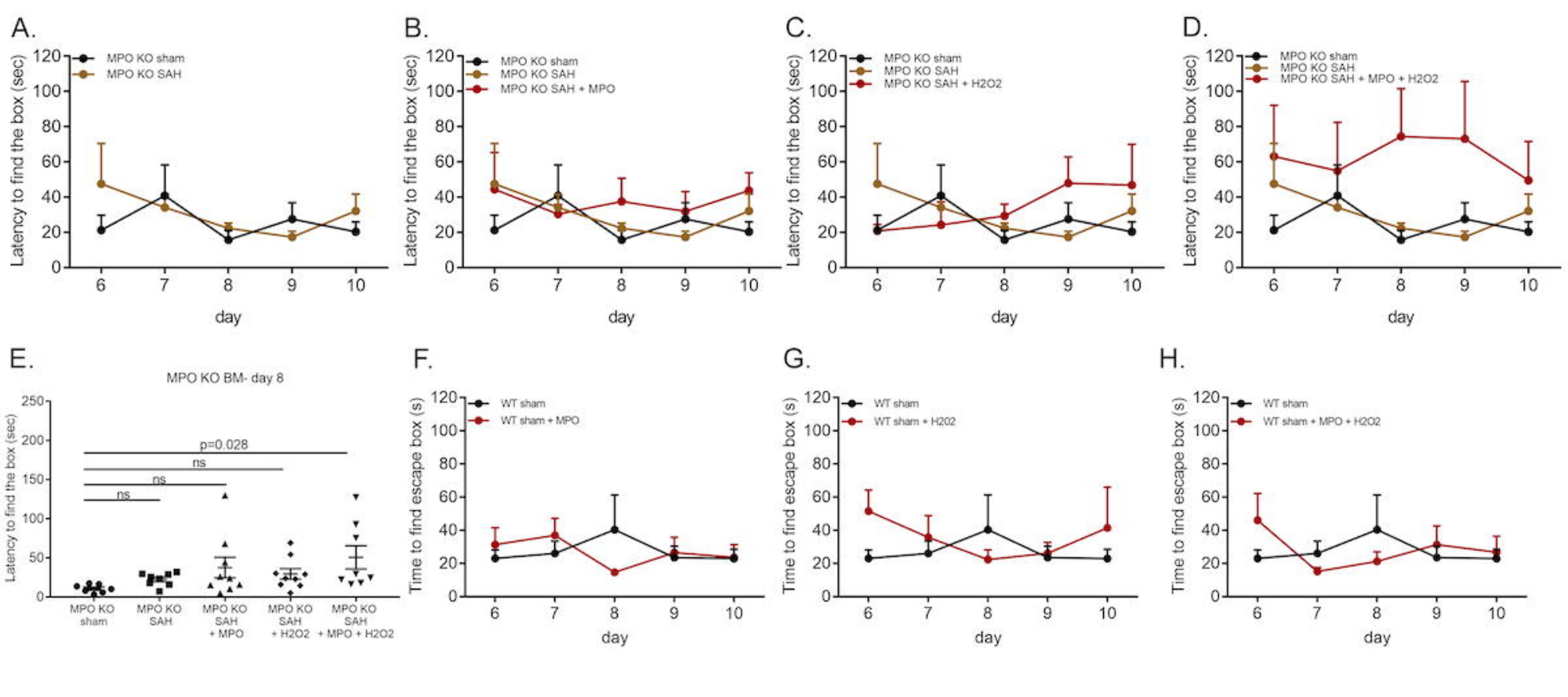
A.
MPO KO sham
MPO KO SAH
Latency to find the box (sec)
day
B.
MPO KO sham
MPO KO SAH
MPO KO SAH + MPO
Latency to find the box (sec)
day
C.
MPO KO sham
MPO KO SAH
MPO KO SAH + H2O2
Latency to find the box (sec)
day
D.
MPO KO sham
MPO KO SAH
MPO KO SAH + MPO + H2O2
Latency to find the box (sec)
day
E.
MPO KO BM- day 8
Latency to find the box (sec)
p=0.028
ns
ns
ns
MPO KO sham
MPO KO SAH
MPO KO SAH + MPO
MPO KO SAH + H2O2
MPO KO SAH + MPO + H2O2
F.
WT sham
WT sham + MPO
Time to find escape box (s)
day
G.
WT sham
WT sham + H2O2
Time to find escape box (s)
day
H.
WT sham
WT sham + MPO + H2O2
Time to find escape box (s)
day

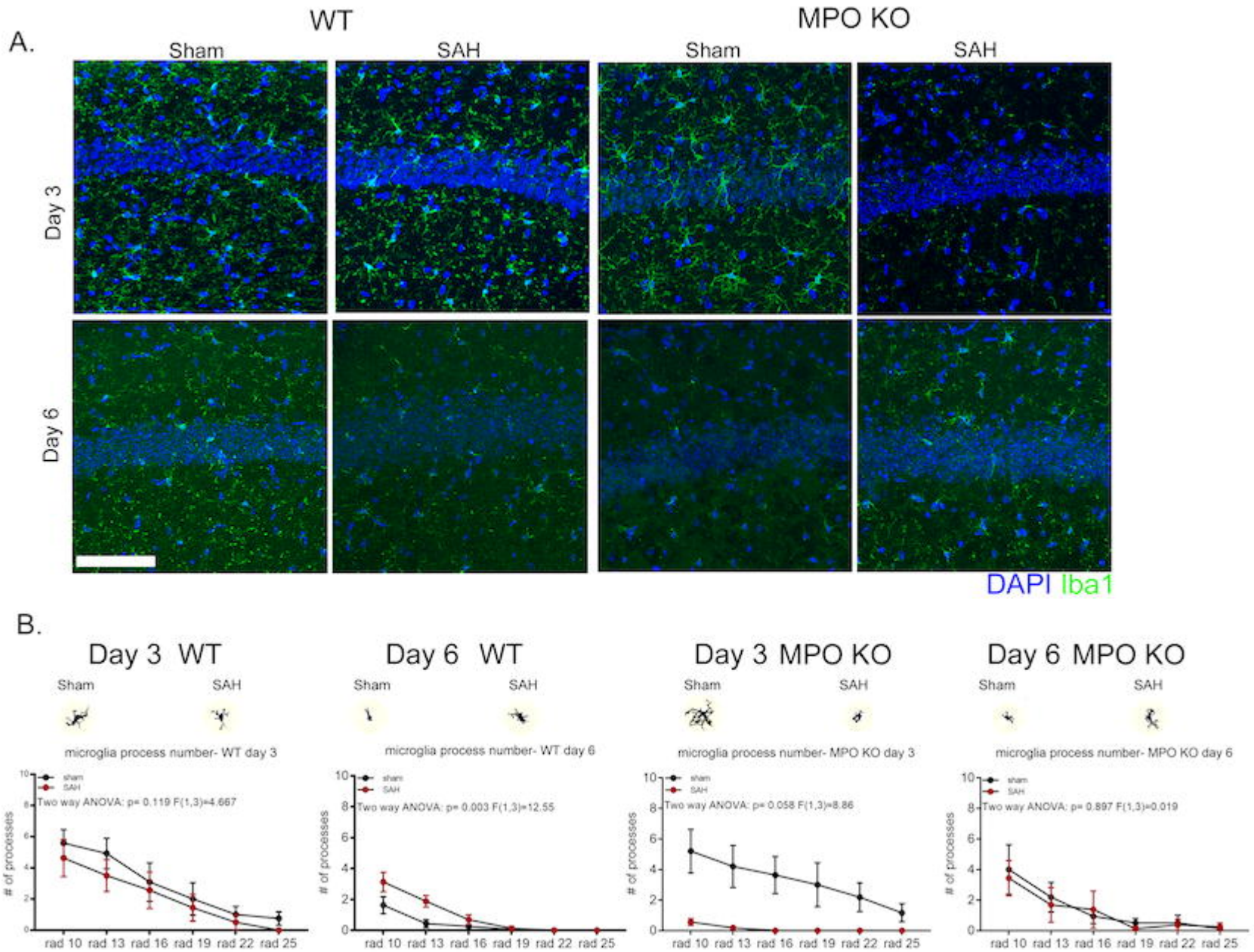
A.
WT
MPO KO
Sham
SAH
Sham
SAH
Day 3
Day 6
DAPI Iba1
B.
Day 3 WT
Day 6 WT
Day 3 MPO KO
Day 6 MPO KO
Sham
SAH
microglia process number- WT day 3
microglia process number- WT day 6
microglia process number- MPO KO day 3
microglia process number- MPO KO day 6
sham
SAH
Two way ANOVA: p= 0.119 F(1,3)=4.667
Two way ANOVA: p= 0.003 F(1,3)=12.55
Two way ANOVA: p= 0.058 F(1,3)=8.86
Two way ANOVA: p= 0.897 F(1,3)=0.019
# of processes
rad 10 rad 13 rad 16 rad 19 rad 22 rad 25

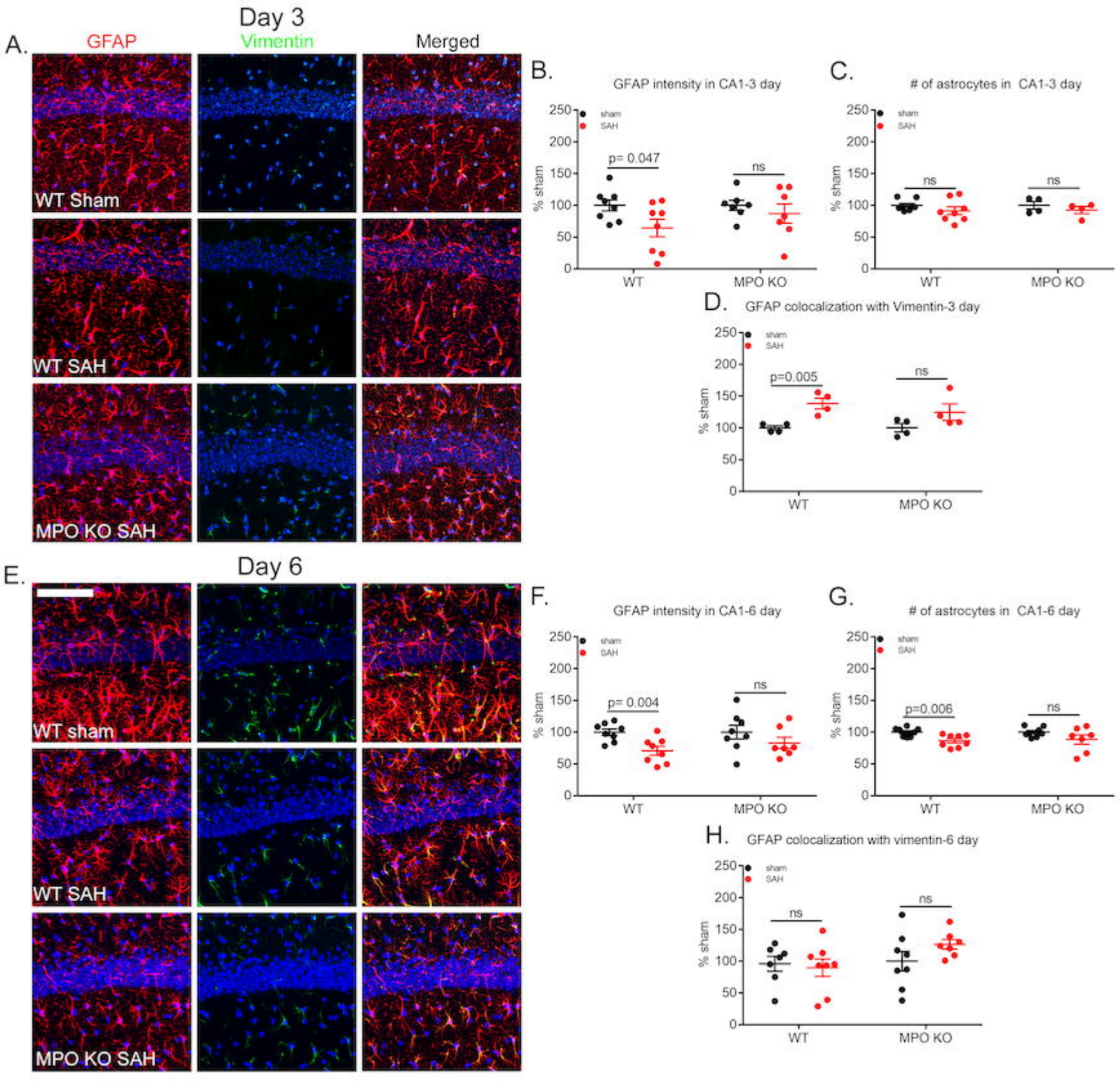
Day 3
A.
GFAP
Vimentin
Merged
WT Sham
WT SAH
MPO KO SAH
B.
GFAP intensity in CA1-3 day
sham
SAH
p= 0.047
ns
% sham
WT
MPO KO
C.
# of astrocytes in CA1-3 day
ns
ns
D.
GFAP colocalization with Vimentin-3 day
p=0.005
Day 6
E.
WT sham
WT SAH
MPO KO SAH
F.
GFAP intensity in CA1-6 day
p= 0.004
G.
# of astrocytes in CA1-6 day
p=0.006
H.
GFAP colocalization with vimentin-6 day